

# Influence of Mg doping on the electronic structure and optical properties of GaN

Y. DU<sup>a,b</sup>, B. CHANG<sup>a</sup>, J. ZHANG<sup>a,\*</sup>, H. WANG<sup>a,c</sup>, B. LI<sup>a</sup>, M. WANG<sup>c</sup>

<sup>a</sup>*Institute of Electronic Engineering and Opto-Electric Technology, NJUST, Nanjing 210094, China*

<sup>b</sup>*Department of Physics, Institute of Bingzhou, Bingzhou, Shandong 256603, China*

<sup>c</sup>*School of Physics, Ludong University, Yantai 264025, China*

The band structure, density of states and E-Mulliken population of wurtzite GaN are calculated systematically before and after Mg doping by using the first-principles plane-wave pseudopotential method, based on the density function theory. The dielectric function, refractive index, absorption spectra, reflective spectra and optical conductivity of wurtzite GaN are analyzed and compared before and after Mg doping. The results show that the Fermi level of GaN comes into the valence band, the density of states shift towards higher energy area, carrier concentration increases significantly; the change of GaN to p-type is achieved after Mg doping. The Mg doping is found to weaken the covalent bond around, and enhance the ionicity and decrease the system stability. It is found that the influence of Mg doping to the optical properties of GaN is greater in visible light area (1.7 ~ 3.1 eV) than in high-energy area. The doping increases static dielectric constant, and enhances photoconductivity.

(Received August 21, 2011; accepted October 20, 2011)

**Keywords:** First-principles, Wurtzite GaN, Electronic structure, Optical properties

## 1. Introduction

GaN is a commonly used as semiconductor materials for a wide range of novel applications in optoelectronic and microelectronic devices. GaN has some fascinating properties such as wide band gap, high thermal conductivity, high breakdown voltage, high melting point and chemical stability. These make it useful for short-wavelength optoelectronic devices, high-temperature devices and high-frequency high-power devices. In recent years, most research focused on its physical properties [1-5]. The optical and electrical properties of optoelectronic materials are mainly characterized by the dielectric function, refractive index, optical conductivity and absorption coefficient. These optical constants are determined by the energy band structure near the Fermi level and the carrier concentrations etc. Consequently, it is necessary to study and calculate the electronic structure of photoelectric materials. The research to the type change of variety of doped photoelectric materials has been a hot issue. Experimental [6-8] and theoretical [9-10] researches have been performed to get p-type or n-type doped GaN material. Undoped GaN is usually n-type conductive material. P-type GaN material could be obtained by Mg doping. Achievement of material makes it is possible to manufacture GaN light-emitting devices. A large number of experiments have proved that Magnesium is a better p-type dopant [11]. In recent years, studies on Mg doping GaN are mainly concentrated on the doping process, electrical properties, etc., but on the influence of Mg doping to optical properties of GaN is few. In this paper,

using the first-principles plane-wave pseudopotential method, on the base of the research on the influence of Mg doping to the band structure, density of states and E-Mulliken population of GaN, dielectric function, refractive index, absorption, reflection spectra, optical conductivity and other optical properties of GaN are analyzed and compared before and after Mg doping.

## 2. Calculation methodology and model

All calculations were performed with the quantum mechanics program *Cambridge Serial Total Energy Package*(CASTEP) [13], based on *density functional theory* (DFT). The *Broyden-Fletcher-Goldfarb-Shanno* (BFGS) algorithm was used to optimize the structure of the crystal model. The valence electronic wave function is expanded in a plane wave basis vector. The final set of energies was computed with an energy cutoff of 400 eV. The convergence precision was set to energy change below  $2 \times 10^{-6}$  eV/atom, force less than 0.005 eV/nm, the convergence tolerance of a single atomic energy below  $1 \times 10^{-5}$  eV/atom, stress less than 0.05 GPa, and change in displacement less than 0.0001 nm in iterative process. All calculations were performed with a plane-wave pseudopotential method based on DFT combined with the *generalized gradient approximation* (GGA) [14,15]. The integral in the Brillouin zone was sampled with the Monkhorst-Pack scheme [16] and special k points of high symmetry. The number of k points is  $7 \times 7 \times 7$ . All calculations were carried in reciprocal space. The wurtzite GaN has a hexagonal structure, which belongs to the

$P63_{mc}$  space group. Symmetry is  $C_{6v-4}$ , the lattice constant can be described with  $a=b=0.3189$  nm,  $c=0.5185$  nm [12],  $\alpha=\beta=90^\circ$ ,  $\gamma=120^\circ$ , where  $c/a$  is 1.626, which is smaller than the ideal hexagonal close packed (HCP) structure 1.633. The Ga-N bond length is 0.1969 nm in  $c$  direction, others are 0.1965 nm. The unit cell is made up by the reverse of *hexagonal close-packed* (HCP) of Ga and N atoms. In calculations  $2 \times 2 \times 2$  supercell of wurtzite GaN was used, composed of 8 GaN unit cells, contains a total

of 32 atoms. One Mg atom replaces one Ga atom in the supercell center; the doping concentration is 6.25%. In calculation experimental data was used for GaN model. The lattice constants of GaN are shown in Table 1 before and after Mg doping. All calculations were carried in reciprocal space with  $Ga:3d^{10}4s^24p^1$ ,  $N:2s^22p^3$  and  $Mg:2p^63s^2$  as the valence electrons. The scissors operator correction was used for the optical properties calculation.

Table 1. The lattice parameters after relaxation.

supercell	a/nm	b/nm	c/nm	v/nm <sup>3</sup>	Minimum energy/eV
GaN	0.32247	0.32247	0.52537	0.3785	-37197.37
GaN:Mg	0.32318	0.32318	0.52759	0.3818	-36117.29

### 3. Results and discussions

#### 3.1. Structural property

The energy band structure of GaN is calculated before and after Mg doping shown in Figs. 1 and 2, in which the dotted line represents the Fermi level. From the band structure, we can see that the conduction band bottom and the top of the valence band of GaN are located in the G point of the Brillouin zone before and after Mg doping, indicating that GaN is a direct band gap semiconductor in these two conditions. Mg atom after doping as acceptors contributes a certain amount of excess charge carriers - holes near the top of the valence band of GaN, making the top of valence band rise from 0eV to 0.184eV and the Fermi level come to valence band. The conduction type of GaN turns into p-type and the band gap width increases from 1.663 eV to 1.831 eV after Mg doping. The exclusionary effect between the energy level in valence band top formed by holes and conduction band bottom formed by Ga4s makes the bottom of conduction band shift to high-energy area, it is why the band gap width increases.

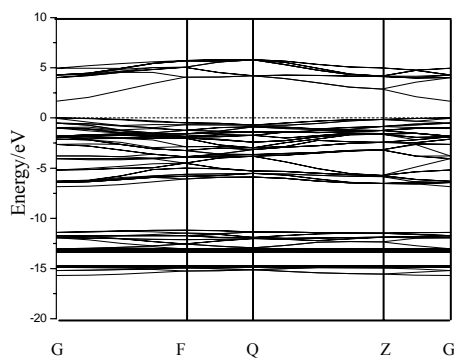


Fig. 1. Energy band structures of GaN.

The band gap calculated above is lower than the experimental value ( $E_g = 3.39$  eV), it is a universal phenomenon when the local density approximation (LDA) and generalized gradient approximation (GGA) have been used in the calculation, but this does not affect the theoretical analysis of the electronic structure of GaN. Another find is that there is a deep acceptor band gap at -39.50 eV after Mg doping.

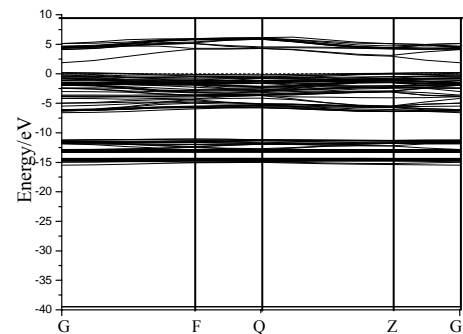


Fig. 2. Energy band structures of GaN:Mg.

#### 3.2 Electronic density of states

It can be seen from Fig. 3 that the valence band of pure GaN is composed of lower valence bands from -15.70 eV to -11.17 eV and upper valence bands from -6.84 eV to 0 eV. The lower valence bands are mainly attributed to Ga3d and N2s state electrons; the upper valence bands are mainly attributed to N2p and Ga4s state electrons; the top of the valence band is decided by N2p state electrons. Conduction bands are mainly attributed to Ga4s and Ga4p state electrons and a small number of N2p state electrons. It can be seen from Fig. 4 that the valence band of GaN after Mg doping is composed of lower valence bands from -15.47 eV to -11.24 eV and upper valence bands from -6.59 eV to 0.18 eV. Peak of density of states near Fermi level is mainly attributed to N2p and Mg2p state electrons hybridization. Since the introduction

of carriers-holes because of high doping concentration so that the Fermi level comes into the valence band so-called Burstein-Moss move, this makes the doped system have the characteristics of degenerate semiconductors and its density of states move to higher energy. There is a peak of density of states in -39.50 eV, which is attributed to Mg2p state electrons; this is in agreement with the results of band structure analysis.

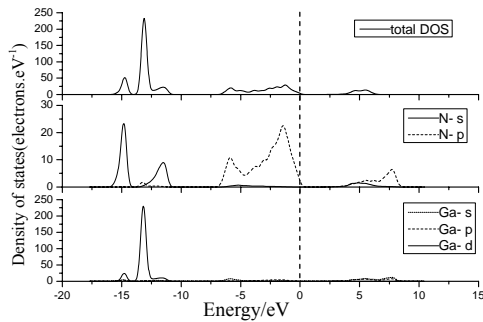


Fig. 3. Partial and total densities of state of GaN.

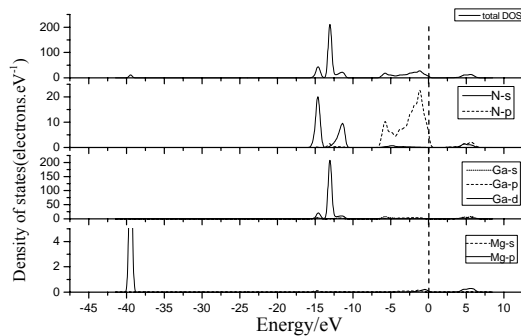


Fig. 4. Partial and total densities of state of GaN:Mg.

The carrier concentrations can be calculated by electronic density of states. After Mg doping, there is electron distribution in conduction band, the concentration of conduction band electrons is calculated as

$$n_0 = \frac{1}{V} \int_{E_c}^{\infty} f(E)g_c(E)dE \quad (1)$$

where  $g_c(E)$  is the density of states near conduction band bottom,  $V$  is super-cell volume.

GaN becomes degenerate semiconductor after Mg doping in high concentration, so the electrons obey Fermi-Dirac distribution

$$f(E) = \frac{1}{1 + \exp\left(\frac{E_i - E_F}{kT}\right)} \quad (2)$$

By integral calculation (integral range from conduction band to the Fermi level) to total density of states (Fig. 4) we can see that, the carrier concentration of GaN after Mg doping is  $3.2 \times 10^{21} \text{ cm}^{-3}$  increasing obviously. This has proved that Mg is a better dopant. It is also found that the exclusionary effect between holes is enhanced with the increase of Mg doping density. The decrease of system stability (see Table 1) leads to the instability of Mg atoms in system, which is why not easy to achieve high quality p-type GaN.

### 3.3 Analysis of E-Mulliken population

Through the analysis of E-Mulliken population, we can understand the bands between atoms, charge distribution, charge transfer and chemical properties of solid. We have calculated the E-Mulliken distribution of GaN before and after Mg doping, the E-Mulliken populations of GaN and GaN : Mg are shown in Table 2. Ga loses  $1|e|$  and N gets  $1|e|$  before doping, the Mulliken population is 0.65 at c-axis direction, bond length is 0.1979 nm, the Mulliken population is 0.57 vertical to c-axis, bond length is 0.1971 nm, covalent bond containing ionic bond is formed between Ga and N. After Mg atom replacing Ga atom, the distribution of charge changes greatly, Mg loses  $1.59|e|$ , as the electronegativity of Mg is very small, N is large, charge distribution of N atoms near Mg atom increases from  $1.0|e|$  to  $1.12|e|$  (along c-axis) and  $1.09|e|$  (vertical to c-axis). The composition of ionic bond paralleling to c-axis is larger than that vertical to c-axis. The Mulliken population along c-axis changes from 0.65 to -0.83, that vertical to c-axis changes from 0.57 to -0.78, -0.78. The bond length along c-axis increases from 0.1979 nm to 0.2067 nm, that vertical to c-axis increase from 0.1971 nm to 0.2061 nm, 0.2062 nm. Doping of Mg weakens covalence and enhances the ionicity.

Table 2. Analysis of E-Mulliken Population of GaN and GaN : Mg.

GaN					GaN:Mg				
Bond	Population	Charge(e)		1/nm	Bond	Population	Charge(e)		1/nm
		Ga	N*				Mg	N*	
Ga <sub>1</sub> -N <sub>2</sub> (cixis)	0.65	1.0	-1.0	0.1979	Mg <sub>1</sub> -N <sub>2</sub> (cixis)	-0.83	1.59	-1.12	0.2067
Ga <sub>1</sub> -N <sub>4</sub>	0.57		-1.0	0.1971	Mg <sub>1</sub> -N <sub>4</sub>	-0.78		-1.09	0.2061
Ga <sub>1</sub> -N <sub>8</sub>	0.57		-1.0	0.1971	Mg <sub>1</sub> -N <sub>8</sub>	-0.78		-1.09	0.2062
Ga <sub>1</sub> -N <sub>16</sub>	0.57		-1.0	0.1971	Mg <sub>1</sub> -N <sub>16</sub>	-0.79		-1.09	0.2061

\* N surround Ga

An abnormal phenomenon is found that the volume after doped increases (see Table 1), that is inconformity with the mechanism that the volume of system after doped should become smaller because the radius of  $Mg^{2+}$  ion is smaller than which of  $Ga^{3+}$  ion. The reason is that the replacement of  $Mg^{2+}$  to  $Ga^{3+}$  leads to lattice distortion. To analyze from band making, the band lengths of Ga-N are in 0.1971 nm ~ 0.1979 nm before Mg doping, which of Mg-N and Ga-N around Mg are in 0.2061 nm ~ 0.2067 nm after Mg doping, this also explains the abnormal phenomenon of volume increase.

### 3.4 Optical properties

#### 3.4.1 Dielectric function of GaN:Mg

Dielectric function as a bridge connecting the microscopic physical transitions and the electronic structures of a solid reflects the band structure of the solid and information about its spectrum. We calculated the complex dielectric function of GaN before and after Mg doping. Figs. 5 and 6 show the changes of complex dielectric function of GaN with the changes of incident photon energy before and after Mg doping, respectively. It can be discovered that the influence of Mg doping to GaN dielectric function is mainly in visible light area (1.7 ~ 3.1 eV) and minimal in the high-energy area. The imaginary part of dielectric function is related to absorption. There are four peaks of the imaginary part of the complex dielectric function  $E_1$ ,  $E_2$ ,  $E_3$  and  $E_4$ . They are 4.5933 eV, 7.6809 eV, 9.2489 eV and 12.6502 eV, respectively. Positions of peaks are in good agreement with the experiment of Kawashima [17]. Among them, the  $E_1$  is generated by the transition of N2p (upper valence band) to Ga4s states,  $E_2$  is generated by the transition of N2p (lower valence band) to Ga4s states,  $E_3$  is generated by the transition of G2p to N2p states,  $E_4$  is generated by the transition of G3d to N2p states. The imaginary part of dielectric function  $\epsilon_2$  has a dielectric peak  $E_5$  in visible light area corresponding energy 2.2289 eV, and becomes smooth and  $E_1$  peak disappears after Mg doping. The peak  $E_5$  is generated by the transition of Mg 2p to Ga4s states. By the Kramers-Kronig dispersion relationship,  $\epsilon_1(\omega)$  can be obtained by integration over a fairly wide frequency range after differential coefficient to  $\epsilon_2(\omega)$ . Therefore,  $\epsilon_1(\omega)$  reaches its maximum and minimum at the maximum slope of  $\epsilon_2(\omega)$  rises and drops respectively and intersects twice with the real axis. It can be obtained from the curve of dielectric function real part that the static dielectric constant of GaN is 3.0695 before Mg doping in agreement with the results calculated by C. Persson [18] not considering phonon interaction. The static dielectric function increases to 5.3143 after Mg doping. Mg doping can increase the static dielectric constant of GaN.

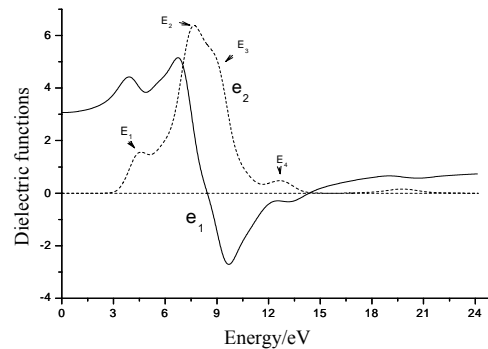


Fig. 5. Complex dielectric functions of GaN.

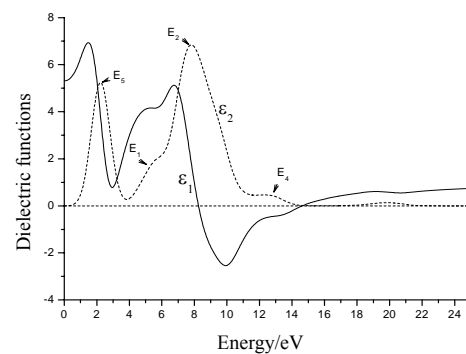


Fig. 6. Complex dielectric functions of GaN:Mg.

#### 3.4.2 Complex refractive index of GaN:Mg

From the relationship of the complex refractive index and the complex dielectric function  $\epsilon_1 = n^2 - k^2$ ,  $\epsilon_2 = 2nk$ , we can obtain the complex refractive index of GaN. Figs. 7 and 8 show the changes of the complex refractive index of GaN with the changes of incident photon energy before and after Mg doping, respectively. It can be discovered that the influence of Mg doping to GaN complex refractive index is large in visible light area (1.7 ~ 3.1 eV). Index  $n$  of GaN increases with incident photon frequency in the energy range of 0 eV ~ 3.1696 eV before Mg doping, shows normal dispersion and is 1.75 in agreement with the results calculated by Li [19]. Index  $n$  of GaN increases with incident photon frequency from 1.75 to 2.30 in the energy range of 0 eV ~ 1.5777 eV after Mg doping and shows normal dispersion. GaN is transparent in this area. Index  $n$  of GaN decreases with the increase of incident photon frequency in the energy range of 1.5777 eV ~ 3.1696 eV after Mg doping and shows anomalous dispersion. In the energy range of 8.2346 eV ~ 14.3629 eV,  $k > n$ ,  $\epsilon_1 < 0$ , light can not propagate in the GaN and GaN shows metal reflective properties. The extinction coefficient  $k$  of undoped GaN shows strong band edge absorption in the low-energy area. Absorption edge is

3.1706 eV corresponding to the transitions of electrons from the top of valance band to the bottom of conduction band. The extinction coefficient  $k$  of GaN after Mg doping has an absorption peak in visible light area, it is corresponding to the peak of imaginary part of complex dielectric function  $\varepsilon_2$ .

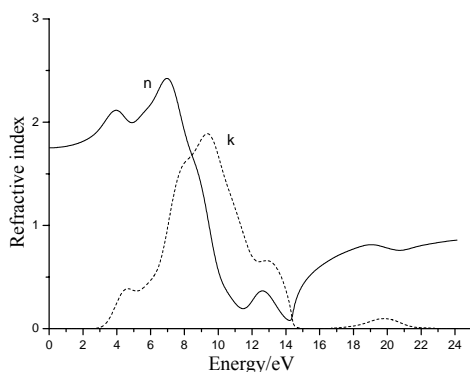


Fig. 7. Refractive index of GaN.

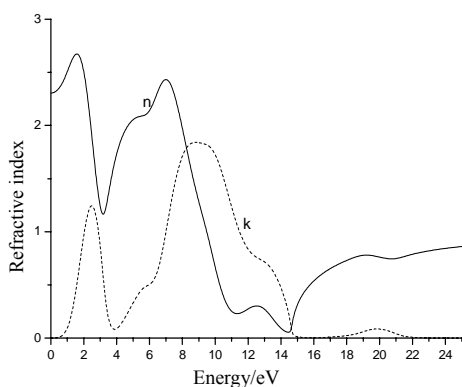


Fig. 8. Refractive index of GaN:Mg.

### 3.4.3 Absorption spectra of GaN:Mg

The light absorption coefficient expresses the percentage of light intensity attenuation per units of distance traveling in the medium. The absorption coefficient of GaN is obtained by  $\alpha \equiv 2\omega k / c = 4\pi k / \lambda_0$  before and after Mg doping and is shown in Fig. 9 (solid line represents before doping, dot line represents after doping). It can be seen that the influence of Mg doping to absorption spectra is large in visible light area (1.7 ~ 3.1 eV). There are four peaks in absorption spectra before Mg doping, the corresponding energies are 4.4968 eV, 9.5264 eV, 13.0121 eV and 19.8388 eV, the maximum of absorption peak is  $287791.4 \text{ cm}^{-1}$  at the energy 9.5264 eV. There has a new absorption peak at the energy 2.8078 eV after Mg doping in visible light area. The disappearing of absorption peak at energy 4.4968 eV is the result of the top of valance band being holes after Mg doping and no

electrons transition to the bottom of conduction band. The peak at energy 19.8388 eV is generated by the transition of Mg3s to Ga4s states. The maximum of absorption peak is  $291842.5 \text{ cm}^{-1}$  at the energy 9.7301 eV, it moves to the high energy of 0.2037 eV.

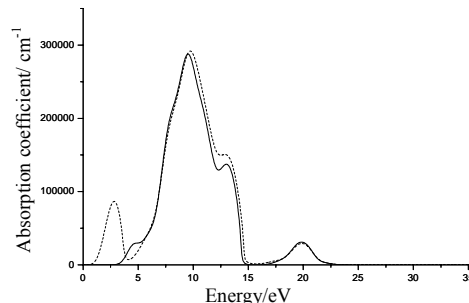


Fig. 9. Absorption coefficient of GaN and GaN:Mg.

### 3.4.4 Reflective spectra of GaN:Mg

When the light is normal incidence to a medium with a complex refractive index from air, so  $n_1 = 1$ ,  $n_2 = n + ik$ . The relationship between the reflective and complex refractive index can be obtained as  $R(\omega) = [(n-1)^2 + k^2] / [(n+1)^2 + k^2]$ . Fig. 10 shows the reflective spectrum of GaN before and after Mg doping (solid line represents before doping, dot line represents after doping). It can be found that the influence of Mg doping to GaN refractive spectra is large in visible light area (1.7 ~ 3.1 eV) and small in the high-energy area. The average value of reflectivity after Mg doping increases from 9.04% to 36.78% in visible light area (1.7 ~ 3.1 eV).

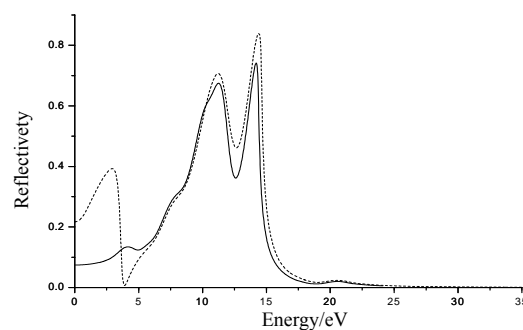


Fig. 10. Reflection spectra of GaN and GaN:Mg.

### 3.4.5 Optical conductivity of GaN:Mg

The optical conductivity of a semiconductor is the change in conductivity caused by illumination and is the physical basis of optoelectronic applications of semiconductors. The optical conductivity of GaN can be obtained by  $\sigma(\omega) = \sigma_1(\omega) + i\sigma_2(\omega) = -i\omega / 4\pi[\varepsilon(\omega) - 1]$  before and after Mg doping and is influenced by Mg doping large in visible light area (1.7 ~ 3.1 eV) as shown

in Fig. 11 (solid line represents before doping, dot line represents after doping). In visible light area, optical conductivity increases significantly, positions of its peaks keep unchanged basically, but curves become smooth. The doping of Mg enhances the optical conductivity of GaN.

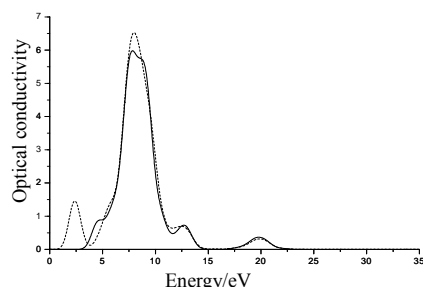


Fig. 11. Optical conductivity of GaN and GaN:Mg.

#### 4. Conclusions

The band structure, density of states, E-Mulliken population and optical properties of wurtzite GaN before and after Mg doping have been calculated based on first-principles plane-wave pseudopotential method. The results show that the Fermi level of GaN comes into valence band, the density of states shifts towards higher energy area, the change of GaN to p-type is achieved after Mg doping. Mg doping is found to weaken the covalent bond and enhance ionicity by analysis to E-Mulliken population. Carrier concentrations of GaN is obtained  $3.2 \times 10^{21} \text{ cm}^{-3}$  after Mg doping by integral to total density of states, it proves that Mg is an ideal dopant. It is found that the influence of Mg doping to the optical properties of GaN is greater in visible light area (1.7~3.1 eV) and small in high-energy area by analysis to the optical properties of GaN before and after Mg doping. Static dielectric constant increases from 3.0695 to 5.3143, and refractive index  $n_0$  increases from 1.75 to 2.30 before and after doping respectively. The optical conductivity increases after doping. Thus, doping is an effective means to modulate the electronic structure and change the optical and electrical properties of materials.

#### Acknowledgments

The authors acknowledge the support of the National Natural Science Foundation of China (Grant No. 60871012), the Shandong Natural Science Foundation (Grant No. ZR2010FL018) and A Project of Shandong Province Higher Educational Science and Technology Program (No. J10LG74).

#### References

- [1] Toru Akiyama, Daisuke Ammi, Kohji Nakamura, Tomonori Ito, Phys. Rev. B, **81**, 245317 (2010).
- [2] G. Kipshidze, V. Kuryatkov, B. Borisov, et al. Appl. Phys. Lett, **80**, 2910 (2002).
- [3] S. T. Li, C. Y. Ouyang, Physics Letters A, **336**, 145 (2005).
- [4] H. X. Wang, B. K. Chang, R. Ling, G. Pin, Appl. Phys. Lett, **98**, 082109 (2011).
- [5] X. H. Wang, B. K. Chang, Y. S. Qian, et al. Optoelectron. Adv. Mater.-Rapid Commun., **5**, 1007 (2011).
- [6] M. Wegscheider, C. Simbrunner, Tian Li, R. Jakiela et al, Appl. Surf. Sci., **255**, 731 (2008).
- [7] Y. Qi, G. F. Sun, M. Weinert, L. Li, Phys. Rev. B, **80**, 235323 (2009).
- [8] Huaibing Wang, Jianping Liu, Nanhui Niu, Guangdi Shen, Shuming Zhang, Journal of Crystal Growth, **304**, 7 (2007).
- [9] A. L. Rosa, J. Neugebauer, Phys. Rev. B, **73**, 205346 (2006).
- [10] Gan, Chee Kwan, Srolovitz, David J., Phys. Rev. B, **73**, 205324 (2008).
- [11] H. Amano, M. Kito, K. Hiramatsu et al. J. Appl. Phys., **28**, 2112 (1989).
- [12] T. Lei, T. D. Moustakas, R. J. Graham, Y. He, S. J. Berkowitz, J. Appl. Phys., **71**, 4933 (1992).
- [13] M. D. Segall, P. J. D. Lindan, M. J. Probert, C. J. Pickard, P. J. Hasnip, S. J. Clark, M. C. Payne, **14**, 2717 (2002).
- [14] J. P. Perdew, A. Zunger, Phys. Rev. B, **23**, 5048 (1981).
- [15] J. P. Perdew, K. Burke, M. Ernzerhof, Phys. Rev. Lett, **77**, 3865 (1996).
- [16] H. J. Monkhorst, J. D. Pack, Phys. Rev. B, **13**, 5188 (1976).
- [17] T. Kawashima, H. Yoshikawa, S. Adachi, S. Fuke, K. Ohtsuka, J. Appl. Phys, **82**, 3528 (1997).
- [18] C. Persson, R. Ahujia, A. Ferreira, et al. Journal of Crystal Growth, **231**, 407 (2001).
- [19] S. T. Li, C. Y. Ouyang. Physics Letters A, **336**, 145 (2005).

\*Corresponding author: zj\_w1231@163.com